# Lawrence Berkeley National Laboratory

**Title**
High-Relaxivity MRI Contrast Agents: Where Coordination Chemistry Meets Medical Imaging

**Permalink**
https://escholarship.org/uc/item/68h1s8g8

**Author**
Werner, Eric J.

**Publication Date**
2008-12-01

# High-Relaxivity MRI Contrast Agents: Where Coordination Chemistry Meets Medical Imaging

*Eric J. Werner, Ankona Datta, Christoph J. Jocher, and Kenneth N. Raymond\**

*The desire to improve and expand the scope of clinical magnetic resonance imaging (MRI) has prompted the search for contrast agents of higher efficiency. The development of better agents requires consideration of the fundamental coordination chemistry of the gadolinium(III) ion and the parameters that affect its efficacy as a proton relaxation agent. In optimizing each parameter, other practical issues such as solubility and in vivo toxicity must also be addressed, making the attainment of safe, high-relaxivity agents a challenging goal. Here we present recent advances in the field, with an emphasis on the hydroxypyridinone family of Gd[III] chelates.*

## 1. Introduction

Magnetic Resonance Imaging (MRI) has become an important technique in modern diagnostic medicine, providing high-quality three-dimensional images of soft tissue without the need for harmful ionizing radiation.[1] Signal intensity in MRI is related to the relaxation rate of *in vivo* water protons and can be enhanced by the administration of a contrast agent prior to scanning. These agents utilize paramagnetic metal ions and are evaluated on the basis of their ability to increase the relaxation rate of nearby water proton spins per concentration of agent administered (i.e. relaxivity). Gadolinium(III), with its high magnetic moment and long electron spin relaxation time, is an ideal candidate for such a proton relaxation agent and is the most widely used metal.[2, 3] Free Gd[III], is toxic ($LD_{50}$ of 0.2 mmol/kg in mice)[4] and must therefore be administered in the form of stable chelates that will prevent the release of the metal ion *in vivo*. For these reasons, the development of ligands for Gd[III], suitable for production of high-relaxivity agents with favorable properties for imaging applications, remains an important goal.

The purpose of this mini-review is to provide a brief summary of changes in the contrast agent field that emphasizes the hydroxypyridinone (HOPO) class of compounds developed by our research group. Principles governing contrast agent efficacy will be discussed with regard to the underlying coordination chemistry of the Gd[III] ion. Highlights will include some of the major conclusions drawn from the background of this field and theory relevant to the rest of the discussion. For a more detailed account of the theory, the reader is referred to several of the excellent reviews on the subject.[1-3, 5] While not intended to be a comprehensive report, several recent attempts to improve agent efficiency through structural modification of the commercially used aminocarboxylate ligands are also presented.

### 1.1. MRI Contrast Agents

Paramagnetic contrast agents enhance the contrast in an MR image by positively influencing the relaxation rates of water protons in the immediate surroundings of the tissue in which they localize.[2, 6] The first experiments to demonstrate the feasibility of such a concept employed manganese(II) salts and achieved tissue discrimination in animal studies.[7, 8] Since these early reports, Gd[III] has become the most widely used metal for the production of paramagnetic contrast agents. The seven unpaired Gd[III] electrons combined with a relatively long electronic relaxation time make this lanthanide effective as a proton relaxation agent. Gd[III] was utilized in the first approved contrast agent in 1988, and while other systems based on Fe-oxide particles and Mn(II) have been approved, Gd-based agents are by far the most commonly used agents in the clinic.[2, 5] It is worth noting that while contrast agents containing Gd[III] increase both the longitudinal and transverse relaxation rates, the percentage change in tissue is much greater for the longitudinal

[*] Dr. Ankona Datta, Dr. Christoph J. Jocher, Prof. Kenneth N. Raymond
Department of Chemistry
University of California
and Lawrence Berkeley National Laboratory
Berkeley, CA 94720
Fax: (+1) 510 486 5283
E-mail: raymond@socrates.berkeley.edu
Homepage: www.cchem.berkeley.edu/knrgrp/home.html

Dr. Eric J. Werner
Department of Chemistry and Physics
Armstrong Atlantic State University
11935 Abercorn Street
Savannah, GA 31419

rate ($1/T_1$). As a result, such agents are best visualized with $T_1$-

*Eric J. Werner received his B.S. degree in chemistry from the University of Florida in 2002. He performed graduate work in the research group of Prof. K. N. Raymond at the University of California, Berkeley (Ph.D., 2007) with a focus on the synthesis and evaluation of high-relaxivity MRI contrast agents. In August 2007, he began his current position of Assistant Professor of Chemistry at Armstrong Atlantic State University in Savannah, GA.*

*Ankona Datta grew up in Kharagpur, India. She received her B.Sc. and M.Sc. degrees in chemistry from the Indian Institute of Technology, Kharagpur, India in 2000. She did her graduate work on chiral water-soluble porphyrins for catalysis and recognition, with Prof. John T. Groves at Princeton University (Ph.D., 2006). Since, 2006 she is a postdoctoral scholar in Prof. Kenneth N. Raymond's group at the University of California, Berkeley, working on macromolecular MRI contrast agents.*

*Christoph Jocher, born in 1976, studied chemistry at the University of Münster where he obtained his PhD with F. Ekkehardt Hahn in 2004 for research on copper coordination chemistry. He moved to the University of California, Berkeley as a postdoc sponsored by the DFG where he focussed on stability determination of lanthanide complexes. Since July 2007 he works for Continental Tires.*

*Professor Kenneth N. Raymond was born on January 7, 1942 in Astoria, Oregon. Following his early education in the public schools of Oregon, he attended Reed College where he received a B.A. in 1964. Following his Ph.D. from Northwestern University, he began his faculty appointment at the University of California at Berkeley on July 1, 1967. There he has remained, becoming Associate Professor in 1974 and Professor in 1978. He was appointed Chancellor's Professor in 2006.*

weighted scans.[2]

The most commonly used commercial contrast agents are shown in Figure 1. All such agents utilize polyaminocarboxylate ligands which incorporate nitrogen and oxygen donor atoms for the Gd$^{III}$ ion. The first six complexes shown in Figure 1 act as nonspecific extracellular agents. Following intravascular injection, these compounds distribute rapidly between plasma and interstitial spaces and are ultimately eliminated via the renal route with half-lives of about 1.6 hours.[9, 10] The remaining three DTPA derivatives, [Gd(EOB-DTPA)($H_2O$)]$^{2-}$, MS-325, and [Gd(BOPTA)($H_2O$)]$^{2-}$, are designed specifically as targeted agents. The BOPTA complex, MultiHance, is known to target the hepatobiliary system and acts as a liver imaging agent,[2, 11, 12] while MS-325 interacts noncovalently with the abundant blood protein Human Serum Albumin (HSA). Once bound to HSA, the proton relaxation efficiency of MS-325 increases and the longer *in vivo* retention times present opportunities for MR angiography.[13-15] Common to all the aminocarboxylate-based commercial agents is the octadentate ligand motif, a chelate design that leaves only one open coordination site for a single inner-sphere water molecule. This low hydration number ($q$) limits the potential effectiveness of these complexes as relaxation agents (*vide infra*).
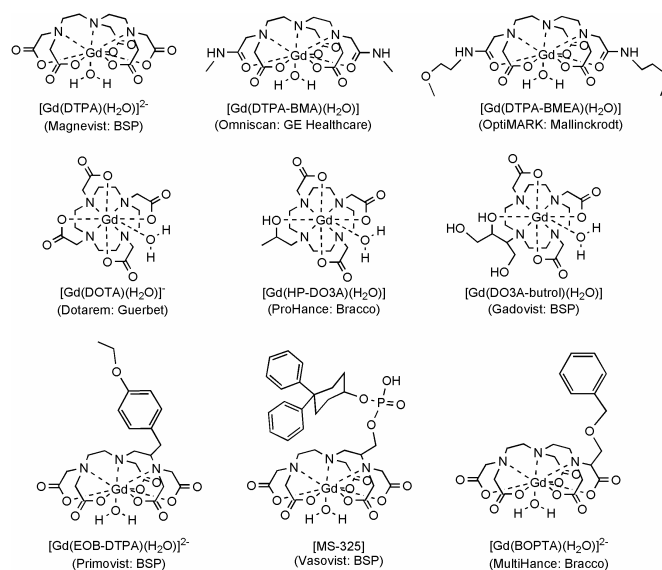


**Figure 1.** Commercial aminocarboxylate-based MRI contrast agents (BSP = Bayer Schering Pharma AG).

## 1.2. Relaxivity and S.B.M. Theory

Contrast agents are evaluated on the basis of their relaxivity, or how much the relaxation rates of water protons are increased in the presence of the agent at a given concentration. The observed relaxation rate of solvent protons, in this case water protons, is comprised of both diamagnetic and paramagnetic contributions. The paramagnetic contribution is linearly related to the concentration of paramagnetic species present. Relaxivity is then defined as the increase in relaxation rate per concentration of the paramagnetic agent, or the slope of a plot of $(1/T_i)_{obs}$ versus concentration ($r_i$, Equation 1).

$$(1/T_i)_{obs} = (1/T_i)_{diamagnetic} + r_i[Gd] \qquad i = 1, 2 \qquad (1)$$

Paramagnetic relaxation enhancement includes both an inner-sphere component from the proton relaxation of a solvent molecule directly coordinated to the Gd$^{III}$ ion, and an outer-sphere component from

solvent in the second coordination sphere and the bulk solvent. Current agent design focuses mainly on attaining higher inner-sphere, longitudinal relaxivity, $r_{1p}$, from protons of water molecules in the first coordination sphere of the metal. Equation 2 reveals that if water exchange at the Gd$^{III}$ center is fast enough (small values of $\tau_M$, the mean water residence time), the paramagnetic relaxation enhancement experienced by the bulk solvent will come from the relaxation rate ($1/T_{1m}$) increase of the coordinated solvent molecule ($1/T_1$ is the longitudinal relaxation rate, $q$ is the number of bound solvent molecules, and $P_m$ is the mole fraction of water coordinated to the metal center). According to the Solomon-Bloembergen-Morgan (S.B.M.) equations of paramagnetic relaxation theory,[16-20] $T_{1m}$ for the applicable dipole-dipole relaxation mechanism is defined by Equation 3. This equation shows that modulation of the correlation time $\tau_c$ defined in Equation 4 becomes critical in the obtainment of the high relaxivities predicted by theory.[2]

$$(1/T_1) = qP_m[1/(T_{1m} + \tau_M)] \quad (2)$$

$$\frac{1}{T_{1m}^{DD}} = \frac{2}{15}\frac{\gamma^2 g^2 S(S+1)\mu_B^2}{r_{Gd-H}^6}\left[\frac{3\tau_{C1}}{1+\omega_H^2\tau_{C1}^2} + \frac{7\tau_{C2}}{1+\omega_S^2\tau_{C2}^2}\right] \quad (3)$$

$$1/\tau_{ci} = 1/\tau_R + 1/T_{ie} + 1/\tau_M \quad i = 1, 2 \quad (4)$$

The relaxivities of current commercial agents based on polyaminocarboxylate scaffolds are small compared to what is theoretically possible, with $r_{1p}$ values of only 4 - 5 mM$^{-1}$s$^{-1}$.[2, 21] As shown by equations 2-4, theory demonstrates the need to maximize the hydration number $q$ ($q = 1$ for all commercial agents) and optimize $\tau_M$ (150 - 1000 ns in commercial agents), the rotational correlation time $\tau_R$ (in the ps regime for small molecules), and the electronic relaxation times $T_{ie}$ to obtain high relaxivity. These parameters are illustrated pictorially in Figure 2, and their optimization can result in a dramatic increase in relaxivity. At 20 MHz, the relaxivity for a $q = 3$ complex can theoretically reach values of above 300 mM$^{-1}$s$^{-1}$, representing a 60-fold increase over the relaxivities of current commercial agents. Such high relaxivities can only be attained, however, if all relevant parameters are optimized. In particular, optimal values of about 1-30 ns for water residence times ($\tau_M$; optimal value decreases with increasing magnetic field strength) and ns values of the rotational correlation time ($\tau_R$) are required to reach the peak in the relaxivity profile. It is therefore necessary to increase water exchange rates and slow down molecular tumbling relative to commercial agents, while also maintaining long electronic relaxation times with a high number of inner-sphere water molecules to achieve the high relaxivities predicted by theory. While attaining a more favorable combination of these parameters relative to current agents is desirable, it must come without sacrificing chelate stability, so that toxicity due to free Gd$^{III}$ is avoided. This clearly presents a challenging problem for the coordination chemist!
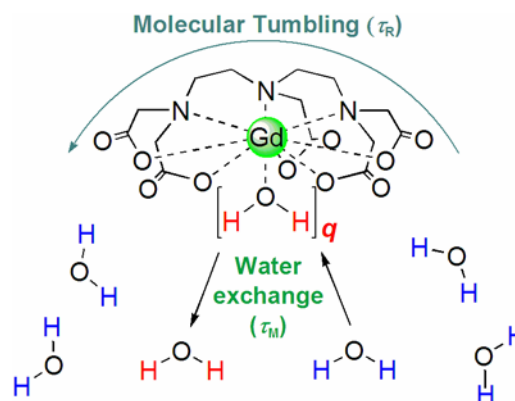


**Figure 2.** Schematic of selected key factors that affect proton relaxivity, $r_{1p}$.

### 1.3. Designing Gd$^{III}$-based Imaging Agents: A Coordination Chemistry Problem

In addition to the favorable electronic properties mentioned above, the general coordination chemistry of the Gd$^{III}$ ion lends itself to its application as a relaxation agent; fast water exchange rates are crucial for attaining high relaxivity, and the ionic radius of Gd$^{III}$ is ideal for fast exchange. Due to lanthanide contraction,[22-25] lanthanide sizes decrease across the 4f row of the periodic table, resulting in higher coordination numbers for the early lanthanides and smaller coordination numbers for those toward the end of the series. Since the Gd$^{III}$ ion is situated in the middle of the row, a low energy barrier exists between the eight- and nine-coordination states, favoring a fluxional state between the two. The rate of water exchange of Gd$^{III}$, once complexed, however, is slowed significantly relative to that of the free ion, often to the extent that it is no longer in the optimal range for high relaxivity. In addition, there is a significant decrease in the number of inner-sphere water molecules as they are replaced by ligating atoms in a chelating ligand.

Related to water exchange, an important trend to consider when designing new contrast agents is relaxation dispersion: the inherent decrease in proton relaxation rates with increasing magnetic field strength.[1, 26, 27] With the appearance of new high field scanners (100 MHz and above) in clinics that give better signal-to-noise ratios this effect becomes significant. Thus, short water residence times (or fast water exchange rates) become increasingly important at high field, with the optimal value for $\tau_M$ decreasing to about 1 ns for 2.4 T scanners (100 MHz proton Larmor frequency). To attain high relaxivities at high fields, the coordination chemistry challenge therefore involves the design of ligands that effectively chelate Gd$^{III}$ while limiting the decrease in the water exchange rate and reduction in $q$ once the ion is bound.

## 2. Recent Strategies in Contrast Agent Design

The primary developmental focus of next-generation MRI contrast agents has been the synthesis of derivatives of the aminocarboxylate systems used in the clinic. Features of compounds such as DTPA and DOTA include inexpensive streamlined syntheses, as well as adequate solubility and toxicological parameters.[1, 28, 29] The following examples illustrate several approaches toward optimizing the aminocarboxylate system en route to more efficient relaxation agents.

Research efforts in new contrast agent design are generally directed towards the optimization of one or more of the aforementioned relaxation parameters through ligand structural modification. For example, Merbach and coworkers have reported numerous studies that probe the factors influencing the water exchange rate of aminocarboxylate Gd[III] complexes.[30-34] The main explanation for increased water exchange rates is steric crowding at the water binding sites, a property that favors the release of the coordinated water molecule in a dissociative exchange process. Derivatives of DTPA, shown in Figure 3, have been synthesized with varying numbers of carbon atoms in the ligand scaffold. As shown by the $\tau_M$ values, water exchange is accelerated in the resultant Gd[III] complexes with values approaching the optimal range for high relaxity at higher magnetic fields (60 – 100 MHz). This rate enhancement is achieved, however, at the cost of thermodynamic stability, as measured by the relatively low pGd[35] values (Figure 3). This phenomenon of decreased stability upon increasing water exchange is common for aminocarboxylate ligands and must be addressed when considering these complexes as high-relaxity agents, particularly at the high magnetic field strengths of future clinical scanners.
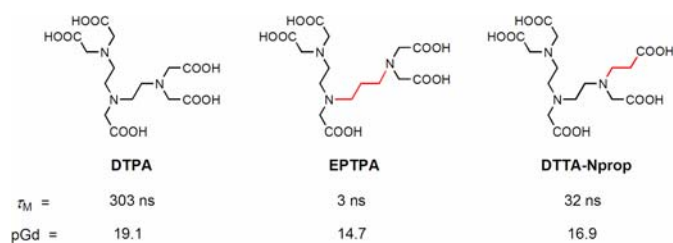


**Figure 3.** The DTPA ligand and two of its representative derivatives prepared for water exchange rate studies.[31, 32]

Increased water exchange rates for macrocyclic complexes based on [Gd-DOTA(H$_2$O)]$^-$ (Figure 1) have also been reported. The pyridine-N-oxide derivative of DOTA (Figure 4) resulted in a Gd complex with a significantly faster water exchange rate than the parent complex ($\tau_M$ of 39 versus 244 ns.[36] ). As with the linear aminocarboxylates mentioned previously, the rate acceleration was attributed to an increase in steric crowding. A monophosphinic acid derivative (Figure 4) was found to possess a faster exchange rate than the parent DOTA complex with a $\tau_M$ of 16.[37] Steric crowding due to the bulky phosphinate group is given as a rationale for the increased rate in addition to a possible favorable arrangement of water molecules in a second coordination sphere. The relaxity of this complex is 6 mM$^{-1}$s$^{-1}$ (20 MHz, 25 °C), an improvement over commercial agents.
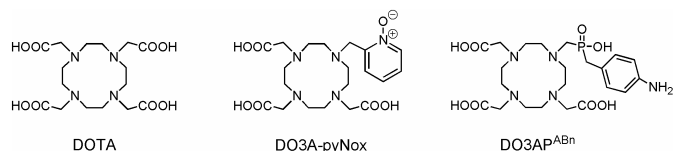


**Figure 4.** The DOTA ligand and representative derivatives prepared to increase water exchange rates.[36, 37]

Complexes with higher $q$ values have also been reported for aminocarboxylate systems in efforts to achieve higher relaxity. As indicated by Equation 2, relaxity is highly dependent on this parameter, and relaxity values will always be limited for complexes that possess only one coordinated water ($q = 1$). Two examples of $q = 2$ complexes are depicted in Figure 5. In each case, DTPA complexes are tethered to a central core to produce dinuclear Gd[III] complexes with increased hydration numbers ($q = 2$). The relaxity values of [Gd$_2$($p$X(DTTA)$_2$)(H$_2$O)$_4$]$^{2-}$ and [Gd$_2$($m$X(DTTA)$_2$)(H$_2$O)$_4$]$^{2-}$ are 12.8 and 11.6 mM$^{-1}$s$^{-1}$ (20 MHz, 37 °C), respectively, and represent significant increases over that of the parent DTPA complex ($r_{1p}$ = 4.3 mM$^{-1}$s$^{-1}$).[2] These values are influenced by the higher $q$ value and (due to increased molecular weight) by an increase in the rotational correlation time, $\tau_R$.[38] A supramolecular approach was used to generate another dinuclear $q = 2$ complex via Fe-terpyridine complexes derivatized with DTPA (Figure 5). The high relaxity of [Fe(tpy-DTTA)$_2$Gd$_2$(H$_2$O)$_4$] (15.7 mM$^{-1}$s$^{-1}$, 20 MHz, 37 °C) is attributed to an increase in $q$ as well as a long $\tau_R$ value resulting from the higher molecular weight and rigidity of the complex.[39]
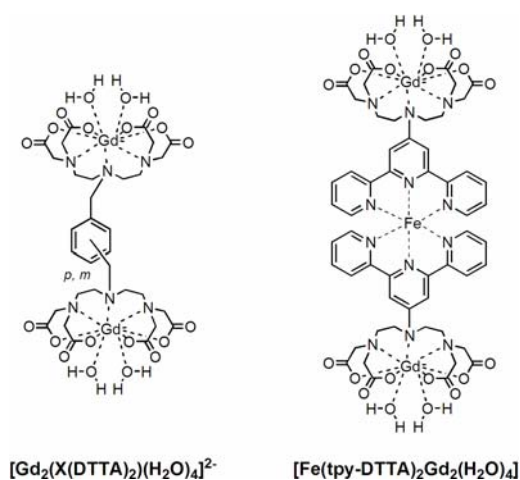


**Figure 5.** Examples of dinuclear, $q = 2$ DTPA-based Gd[III] complexes proposed as improved high-relaxity MRI contrast agents.[38, 39]

While the relaxometric properties of such $q = 2$ compounds are improved, the thermodynamic chelate stability suffers greatly in both cases. The increase in $q$ (Figure 5) from one to two is made possible by removing one carboxylate arm of the parent DTPA to open up a metal coordination site. As is observed in accelerating water exchange in the aminocarboxylate class of compounds, attaining a higher number of coordinated water molecules by decreasing ligand denticity is accompanied by a dramatic decrease in thermodynamic stability. The pGd values for the $p$- and $m$-substituted xylene-based complexes, 16.2 and 15.1, respectively, are significantly lower than the value of 19.1 for the parent DTPA complex.[28] Even less stable is the Fe-terpyridine complex; its pGd value of 10.6 represents more than a 5 log unit decrease in stability relative to DTPA-BMA (pGd = 15.8) (Figure 1), the ligand with the lowest pGd value of all clinically approved agents. This effect of decreased stability upon increasing $q$ or water exchange rates raises a key concern in contrast agent design: The optimization of one parameter will often hamper that of another, making the goal of high-relaxity, practical agents a major challenge. To achieve a practical high-relaxity agent, the optimal combination of all relevant parameters must be accomplished while maintaining solubility and chelate stability.

4

As an example of a Gd-based contrast agent not focused on traditional aminocarboxylate ligand scaffolds, Wilson and coworkers have reported several studies of Gd$^{III}$ encapsulated inside fullerene cages.[40-42] The peripheries of these cages are decorated with solubilizing groups to allow for application of C$_{60}$ in aqueous media. Relaxivities ranging from about 10 to as high as 38.5 mM$^{-1}$s$^{-1}$ (30 MHz, 26 °C) are due entirely to second and outer-sphere relaxation, as there are no inner-sphere waters directly coordinated to the Gd. In solution, these "gadofullerenes" aggregate, resulting in large assemblies with long rotational correlation times and consequent high relaxivities.[42] However, practical concerns such as *in vivo* toxicity and deaggregation in the presence of various salts (thereby limiting the effect of long $\tau_R$ values on relaxivity)[43] may preclude considering such systems for contrast agent applications.

# 3. Hydroxypyridinone-based agents

In 1995, Raymond and coworkers reported a Gd$^{III}$ complex that showed promise as a contrast agent, Gd-TREN-1-Me-3,2-HOPO (**1**, Figure 6).[44] The X-ray crystal structure revealed that the TREN (tris-(2-aminoethyl)-amine) capped tripodal hydroxypyridinone (HOPO) ligand is hexadentate, leaving two open water coordination sites in its overall 8-coordinate complex. The $r_{1p}$ value of this complex, 10.5 mM$^{-1}$s$^{-1}$ (20 MHz, 37°C), is more than twice that of commercial agents. This observed increase is due in large part to a $q$ value of 2, a quantity double that of current commercial agents, combined with a rapid water exchange rate. Even more important and unlike that of previous $q = 2$ complexes, the stability of this complex is higher than that of commercial agents despite the lower ligand denticity (pGd = 19.2[45]). This can be attributed in part to the exclusively oxygen donor set provided by the HOPO chelates (instead of the mixed oxygen/nitrogen donors of the aminocarboxylates) since lanthanide cations prefer hard, anionic oxygen donors to nitrogen.

Since this initial report, a family of HOPO-based Gd complexes has been developed to explore the potential of this motif as MRI contrast agents.[46] Early studies were hindered by the low aqueous solubility of the parent TREN-1-Me-3,2-HOPO complex,[47, 48] which led to subsequent effort to improve this important parameter. The bis-HOPO-TAM motif (replacement of one HOPO unit with a terephthalamide (TAM) chelator) was introduced (**2**, Figure 6) to create a negatively-charged Gd$^{III}$ complex.[47] A key feature of this

ligand design is the second amide functionality of the TAM that allows for further derivatization with solubilizing and targeting groups.[49, 50] Relaxivities of Gd-HOPO and bis-HOPO-TAM complexes are generally in the range of 7 – 13 mM$^{-1}$s$^{-1}$ (20 MHz), and high complex stabilities combined with increased $q$ and optimal water exchange rates make these compounds promising as safe, high-relaxivity agents at high field. The coordination chemistry and relaxometric properties of this class of compounds will be described in the following sections with emphasis on recent work published subsequent to a previous review.[46] Additionally, a detailed summary of the solution thermodynamic stability and selectivity data collected thus far is presented for this class of potential MRI contrast agents.

## 3.1. Solution Thermodynamics

High stability is essential for gadolinium chelate complexes used in medicine due to toxicity related to the presence of free Gd$^{III}$ *in vivo*. For example, precipitation of the metal can occur in tissue, and hydrated lanthanide ions are known to block Ca$^{2+}$ binding sites.[28] When one considers other potential interactions with various serum proteins, as well as irreversible binding to skeletal tissue that can occur with free Gd$^{III}$,[2] the importance of the chelate staying intact while in the body becomes clear. Utilizing the known oxophilicity of lanthanides, purely oxygen donor ligands such as hydroxypyridinone (both the 3,2-HOPO and 1,2-HOPO isomers), maltol (MAM), and terephthalamide (TAM) have been developed and explored as chelators expected to form stable Gd complexes. The obtained complexes (with two[46] or three[51] inner-sphere water molecules) have been examined as candidates for next generation agents. The feasibility of applying these O donor ligands as practical agents has been proven successfully *in vivo*.[52] Scaffold and chelate group variations were also examined to help understand the principles governing stability aspects. The results obtained from these solution thermodynamic studies are summarized in the following sections.
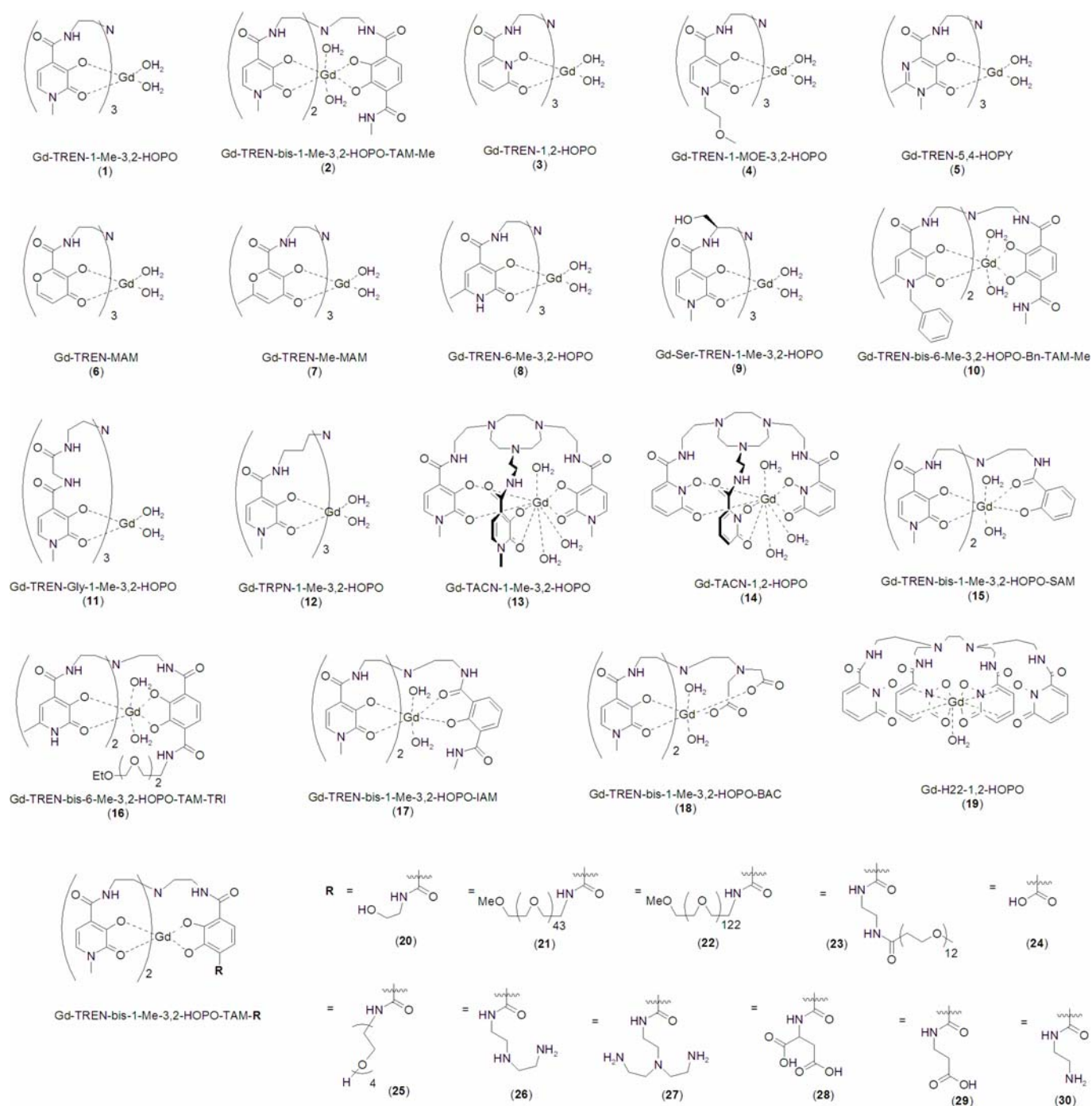
**Figure 6.** Chemical structures of HOPO-based Gd[III] complexes discussed in this paper.

*Stability Constants*

Thermodynamic stability data of HOPO-based chelates have been published. Typically, stabilities of MRI contrast agents are reported as their pGd values, thus providing a convenient way to compare stabilities of chelates with differing protonation behavior.[2, 53] These pGd values range from 13.7 to 20.6 (see Table 1) for hexadentate ligands, and one octadentate ligand achieves a pGd 21.2. For comparison, the benchmark compounds DTPA and DOTA reach 19.1[2, 28] and 20.4,[54] respectively, while DTPA-BMA has the lowest value of all approved agents at 15.8.
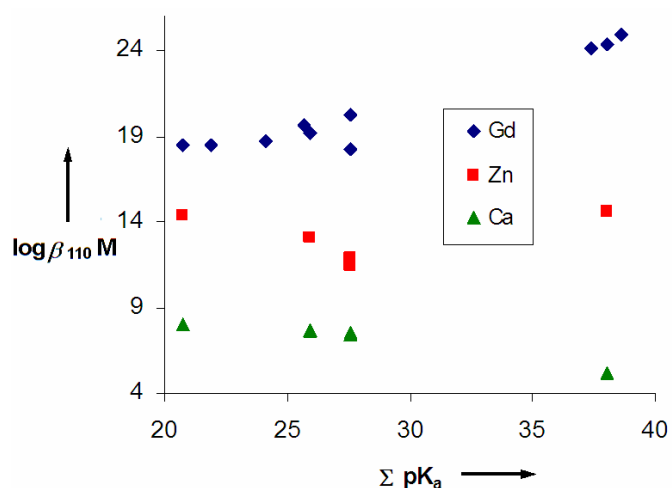
**Figure 7.** Metal binding constants for Gd^III, Zn^II, and Ca^II versus ligand acidity of a series of TREN ligands (Table 1, entries 1 through 10 for Gd^III). The symbols of diamonds, squares, and triangles correspond to binding constants for Gd, Zn, and Ca, respectively.

The favorable thermodynamic properties of HOPO ligands can be attributed to several effects. First, the Gd^III cation is highly oxophilic and will bind more strongly to the six oxygen donors of the HOPO-based ligands than the mixture of nitrogen and oxygen donors offered by hexadentate aminocarboxylate ligands. Second, the two donor atoms on each HOPO moiety are predisposed to bind Gd^III in a five-membered chelate ring. Such an arrangement of donor atoms is expected to favor larger cations such as Ca^II or Gd^III over smaller cations such as Zn^II and Cu^II.[55-57] The final important effect is that the Lewis basicities of the HOPO oxygen donor atoms are an optimal match for Gd^III, resulting in strong binding.[45, 55, 56]

*Scaffold*

A significant factor in chelate stability is the ligand cap scaffold. The TREN scaffold has been found to provide the highest chelate stability for hexadentate HOPO ligands. For example, in a series of 1-Me-3,2-HOPO ligands, replacing TREN[45] with the propylene-bridged cap TRPN (**12**),[58] extending TREN via insertion of three Gly spacers into the ligand arms (**11**),[58] or variation towards a more sterically crowded Ser-TREN (**9**)[59] reduces pGd from 19.2 to 16.7, 15.6, and 17.7, respectively. Complex **12** demonstrates the importance of an intramolecular hydrogen-bonding network which preorganizes the ligand for metal complexation in the TREN-capped complexes such as **1**.[44, 60, 61] The extension of the spacer in TRPN disrupts these interactions, resulting in a lower pGd. While most deviations from the TREN cap have resulted in significantly decreased stability, an exception is the TACN (triazacyclononane) scaffold (**13**) which attains a similar pGd = 18.7.[51]

**Table 1.** Ligand acidity, Gd^III binding constants $\log\beta_{110}$ (in 0.1 M KCl at 298 K) and pGd values of various HOPO-based chelate systems. The top section summarizes TREN capped ligands, and the remaining ligands are listed at the bottom.

| Σ pKa | $\log\beta_{110}$ | pGd[b] | Compound (number from Figure 6) | Ref |
|---|---|---|---|---|
| 20.70 | 18.5 | 19.3 | TREN-1,2-HOPO (3) | 69 |
| 21.90[a] | 18.5[a] | 19.3[a] | TREN-MAM (6) | 63 |
| 24.15[a] | 18.7[a] | 19.0[a] | TREN-Me-MAM (7) | 63 |
| 25.69 | 19.7 | 19.8 | TREN-1-MOE-3,2-HOPO (4) | 48 |
| 25.96 | 19.2 | 19.2 | TREN-1-Me-3,2-HOPO (1) | 45 |
| 27.57 | 18.2 | 18.0 | TREN-5,4-HOPY (5) | 67 |
| 27.61 | 20.3 | 19.5 | TREN-6-Me-3,2-HOPO (8) | 45 |
| 37.34 | 24.1 | 20.1 | TREN-bis-1-Me-3,2-HOPO-TAM-Me (2) | 47 |
| 38.05 | 24.3 | 20.3 | TREN-bis-1-Me-3,2-HOPO-TAM-EA (20) | 66 |
| 38.64 | 24.9 | 20.6 | TREN-bis-6-Me-3,2-HOPO-TAM-PEG₃Et (16) | 62 |
| 24.52 | 15.9 | 16.7 | TREN-Gly-3,2-HOPO (11) | 58 |
| 24.77 | 17.2 | 17.7 | Ser-TREN-3,2-HOPO (9) | 59 |
| 26.59 | 16.5 | 16.2 | TREN-bis-3,2-HOPO-IAM (17) | 47 |
| 26.59 | 14.8 | 13.7 | TREN-bis-3,2-HOPO-BAC (18) | 47 |
| 27.53 | 16.5 | 15.6 | TRPN-1-Me-3,2-HOPO (12) | 58 |
| 28.13 | 17.3 | 16.1 | TREN-bis-3,2-HOPO-SAM (15) | 47 |
| 37.11 | 21.5 | 21.2 | H(2,2)-1,2-HOPO (19) | 65 |

[a] 0.1 N NaCl [b] pH = 7.4; $c_M^{tot}$ = 1 μM; $c_L^{tot}$ = 10 μM.

*Acidity*

Variations in the chelate groups influence pGd values only to a minor extent in the examined TREN-capped hexadentate, homopodal ligands. TREN-3,2-HOPO (**1**), TREN-MAM (**6**), TREN-1,2-HOPO (**3**), TREN-1-MOE-3,2-HOPO (**4**), and TREN-6-Me-3,2-HOPO (**8**) all have similar pGd values falling in the range of 19.2 – 19.8, values that slightly exceed the benchmark compound Gd-DTPA (19.1). The only notable exception is TREN-5,4-HOPY (**5**), with a lower pGd of 18.0. Significant differences across the series appear more clearly, however, when considering log $\beta$ values and protonation constants for a series of TREN-HOPO based complexes (Table 1 and Figure 7). The log $\beta$ values for Gd^III binding increase with the increasing ligand basicity for the series.

The pGd value varies with pH and a plot of pGd versus pH can indicate the acid resistance of the Gd^III complex (Figure 8). The more acidic TREN-1,2-HOPO ligand has greater resistance to acid hydrolysis, when compared to Gd-DTPA. In comparison, the more basic TREN-3,2-HOPO ligand forms a Gd complex that is more acid-sensitive than both DTPA and Gd-TREN-1,2-HOPO. The variation of pGd with pH for a particular Gd^III complex can thus give useful information about the stability of the complex under different pH conditions *in vivo*. In considering targeted imaging, such information can serve as an important guide when designing agents for a specific region of a particular pH.
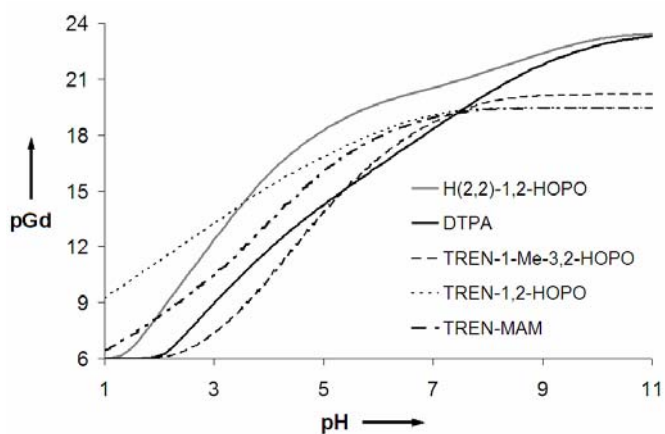
**Figure 8.** Ligand acidity influences the acid resistance of the complex. Basic 1-Me-3,2-HOPO chelates tend to be slightly more sensitive to acid than DTPA, while acidic 1,2-HOPO and MAM ligands form more stable Gd$^{III}$ complexes under acidic conditions than DTPA.

### Charge

The influence of the overall charge of the Gd$^{III}$ complex on the stability constant pGd is demonstrated in a series of eight TREN-bis-3,2-HOPO-TAM chelates (**23 – 30**). Varying the substituent on the TAM moiety and consequently the complex charge resulted in pGd values ranging from 17.1 (-3 charge) to 19.9 (neutral).[64] Interestingly, the three anionic complexes of –1 charge (**23**, **25** and **30**) all exhibit the same pGd value. This study demonstrated that, to maximize stability, the charge of the complex should be as close to zero as possible, with the highest pGd belonging to the neutral amine substituted complex **26**.

### Selectivity

For Ca$^{II}$ and Zn$^{II}$ binding, no clear trend between ligand acidity and binding strength is seen in the data shown in Figure 7. The more basic ligands have a higher selectivity for Gd$^{III}$ over Zn$^{II}$ and Ca$^{II}$, as indicated by the differences in the pM values illustrated in the following examples. The two more basic TREN-bis3,2-HOPO-TAM ligands (**20 and 25**) prefer Gd$^{III}$ by Δp(Gd-Zn) = 8.1 and 7.0,[64, 66, 68] while the relatively less basic TREN-1-Me-3,2-HOPO (**1**) achieves a selectivity of Δp(Gd-Zn) = 6.1,[44, 45] all of which exceed that of DTPA (Δp(Gd-Zn) = 4.2). The Gd$^{III}$ selectivity of the most acidic ligand, TREN-1,2-HOPO (**3**), is the lowest (Δp(Gd-Zn) = 4.1) among the ligands studied.[69] Increasing denticity from six to eight improves the discrimination behavior for 1,2-HOPO to Δp(Gd-Zn) = 6.7 in the case of H(2,2)-1,2-HOPO (**19**).[65]

### Solution Anion Affinity

Solution serum anion affinities of an anionic (**25**) and a cationic (**27**) TREN-bis-1-Me-3,2-HOPO-TAM complex ($q = 2$) are comparable to commercial contrast agents ($q = 1$).[64] Phosphate binds weakly with logK$_A$ = 1.4 and 2.4, respectively. Oxalate is the only other physiologically relevant anion that interacts (logK$_A$ = 1.0 and 2.9) with these complexes. These affinities are similar to the phosphate binding values of the commercial contrast agents DTPA

(logK$_A$ = 2.0) and DOTA (logK$_A$ = 2.2), while aminocarboxylate ligands with $q = 2$ such as DO3A exhibit higher anion affinities (logK$_A$ = 4.8).[6] In comparing the HOPO complexes with DO3A, this difference in anion binding despite the same hydration number ($q = 2$) illustrates the importance of coordination geometry. In the case of **25** and **27**, it is proposed that the water molecules are in positions anti with respect to one another, making it more difficult to displace both waters. Interestingly, the oxalate binding for the cationic chelate **27** increased the coordination number from eight to nine, but no change in coordination number occurred for the anionic chelate **25** since the oxalate replaces both bound water molecules.[64] Neutral TREN-1,2-HOPO (**3**), which contains the more acidic chelate 1,2-HOPO, exhibits a small affinity for oxalate (logK$_A$ = 1.5) and an interaction with a bidentate 3,2-HOPO anion could be detected (logK$_A$ = 3.5) For both the oxalate and bidentate 3,2-HOPO anions, an increase in coordination number was observed by relaxivity and, in the case of oxalate, by luminescence measurements of the Eu(III) analog. No phosphate binding, however, could be detected for this ligand.[69] Octadentate H(2,2)-1,2-HOPO (**19**) does not show any anion binding at neutral pH in which the neutral, monoprotonated complex GdLH complex dominates.[65] Thus, the HOPO-based ligands examined do not have any appreciable anion binding for the physiologically relevant anions that could affect the *in vivo* performance of these ligands.

### In Vivo Behavior

The biodistribution of several of the HOPO-based chelates was tested in mice.[52] Depending on the functionalizing groups of the chelates, different accumulation locations and finely tuned retention times were observed. For example, liver uptake is enhanced upon addition of a short polyethylene glycol (PEG) chain to the chelate, while longer PEG chains favor blood pool localization. Complex **22**, bearing a relatively long chain of 123 ether units, gave the best MR angiographic results despite the known decrease in human serum albumin (HSA) affinity with increasing PEG chain length.[50] In this case, the low albumin affinity may enhance the MR angiogram quality by limiting water displacement from the Gd center by the protein.

### 3.2. Tuning q and water exchange

As most HOPO-based Gd$^{III}$ complexes are 8-coordinate, an associative water exchange mechanism involving a 9-coordinate intermediate species can be predicted. The energy difference between the 8-coordinate ground state and a 9-coordinate intermediate is small, leading to fast water exchange and subsequent high relaxivity (Figure 9).[62, 70] This rapid exchange rate was initially supported by temperature-dependent relaxivity studies and the X-ray crystal structure of the La-TREN-1-Me-3,2-HOPO complex. In this structure both an 8- and a 9-coordinate metal center are observed.[47] The presence of both coordination numbers indicates that the coordination environments of the two lanthanide ions must be similar in energy and that the ligand motif can accommodate both. Indeed, variable pressure $^{17}$O NMR studies have been carried out for Gd-TREN-bis-6-Me-3,2-HOPO-TAM-TRI (**16**) to determine a small, negative value for the volume of activation, a result indicative of associative interchange exchange.[62]
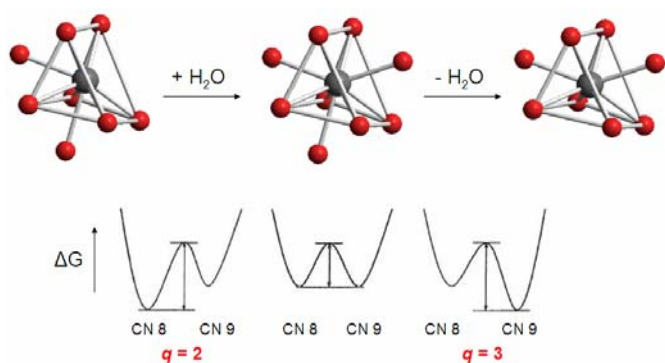
**Figure 9.** Top: coordination polyhedra of the Gd ion illustrating associative water exchange for HOPO-based complexes. Bottom: free energy diagrams for water exchange.[47] Most HOPO complexes have an 8-coordinate ground state and a 9-coordinate intermediate (left) but studies indicate both states are close in energy.

Since the eight- and nine-coordinate states are close in energy for Gd-HOPO complexes, small changes in the ligand structure can affect the number of bound water molecules ($q$) and the rate of water exchange. Importantly, increases in $q$ of HOPO-based complexes have been accomplished without reducing the denticity of the ligand, resulting in complexes with fast water exchange rates that maintain the favorable thermodynamic stability properties of the parent compound. The following section reviews several examples that demonstrate the effect of both ligand scaffold and substituent on water coordination in the HOPO family of Gd$^{III}$ complexes.

*Effect of PEG Substituents*

Utilization of the TREN-bis-HOPO-TAM motif as in complex **2** affords negatively charged Gd complexes and a modest increase in aqueous solubility relative to the parent complex **1**. In order to further enhance solubility of HOPO-based complexes, polyethylene glycol (PEG) chains were introduced to the bis-HOPO-TAM design. Additionally, it was proposed that the PEG moiety may induce noncovalent interactions with the abundant blood protein HSA to slow tumbling (higher $\tau_R$) and thereby increase relaxivity.[49] The first PEGs chosen for attachment were chains of 44 (**21**) and 123 (**22**) ether moieties. Analysis of the NMRD profiles of complexes **21** and **22** indicate a reduction in $q$ relative to the parent $q = 2$ complex **2**, with the best refinements obtained by fixing $q$ to a value of 1. This can be explained by the ether oxygen atoms partially coordinating to the Gd center, displacing bound water molecules. Variable temperature $^{17}$O NMR experiments were conducted to yield the water exchange rates of each complex. It was noted that $\tau_M$ increases as the PEG chain is lengthened, enabling tuning of the rate. A reduction in the hydration number for PEG-substituted complexes has also been observed in subsequent studies.[50] While complexes bearing chains of 11 and 12 ether units (**23**) exhibit relaxometric behaviour that suggests $q = 1$,[50, 64] $q$ remains 2 as in the parent compound when the chain is reduced to 4 ethers (**25**). These results indicate that a relatively short PEG chain is necessary to balance a high $q$ value with water solubility.

*Effect of non-PEG Solubilizing Substituents*

In addition to the PEG-substituted compounds, bis-HOPO-TAM complexes bearing alcohols, acids, and amines have been studied with regard to their effects on water coordination. In a recent study,

tuning of the coordination number was demonstrated by the addition of pendant amine groups. At physiological pH, one such substituent forms a hydrogen bond interaction with a water molecule, thereby favoring its coordination (Figure 10). This results in a stabilization of the nine-coordinate, $q = 3$, state in the exchange process, and a consequent higher relaxivity (11.1 mM$^{-1}$s$^{-1}$; 20 MHz, 298 K, pH 7).[70] Importantly, the complex (**30**) retains high stability as indicated by the pGd value of 19.4, comparable to [Gd(DTPA)]$^{2-}$, as well as high relaxivity at the relevant magnetic field strengths above 0.5 T.
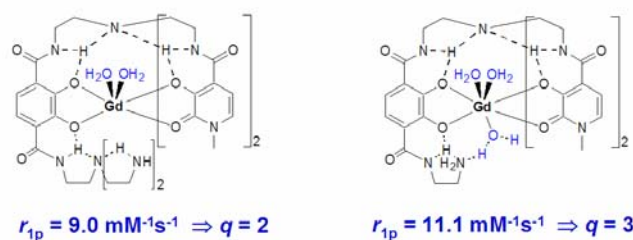


**Figure 10.** TREN-bis-HOPO-TAM complexes (**27** and **30**) substituted with pendant amines. The complex (**30**) shown on the right possesses a substituent capable of forming a hydrogen bond with an additional water molecule to promote its coordination to the Gd$^{III}$ center.

Further study of other solubilizing substituents demonstrated the abilities of other structures to partake in similar hydrogen bond interactions to aid in water binding at the metal center. Complexes bearing the ethanolamine moiety (**20**) and various carboxylic acid groups (**28** and **29**) also have relaxometric properties consistent with three bound water molecules as indicated by NMRD profiles.[64] In all cases, thermodynamic stabilities were determined to be sufficient for consideration of such compounds as clinical agents. Also noteworthy is that the water molecule residence times obtained for the series of complexes are all similarly short, regardless of complex charges or ground state coordination numbers. This observation provides further support for the closeness in energy of the eight- and nine-coordination states for HOPO-based complexes and reveals how subtle changes in ligand structure can alter the nature of the ground state (Figure 9).

*TACN-capped Complexes*

The effect of the ligand-capping structure on water coordination has also been explored. In a recent report, triazacyclononane (TACN) was used as a ligand cap to produce both tris-3,2- and 1,2-HOPO complexes (**13** and **14**).[51] Molecular modelling studies predicted that the larger cap (relative to TREN) would accommodate three inner-sphere water molecules, and subsequent relaxometric and luminescent characterization revealed a successful design strategy. Relaxivities were found to be 13.1 and 12.5 mM$^{-1}$s$^{-1}$ (20 MHz, 298 K, pH 7), values that remained high at field strengths above 0.5 T. The stabilization of the $q = 3$ complex in this case is accomplished without the need for the asymmetric bis-HOPO-TAM motif. Use of the TACN cap also results in a dramatic increase in aqueous solubility, possibly due in part to protonation of the TACN cap resulting in a charged species near neutral pH. Furthermore, stability is not significantly affected (pGd = 18.7) upon increasing the hydration number to $q = 3$. These TACN-capped complexes are therefore unique examples of highly soluble tris-HOPO Gd$^{III}$

complexes that demonstrate high hydration numbers, fast water exchange rates, and high stabilities.

### 3.3. Increasing rotational correlation times through macromolecular association

Once the basic hydration and water exchange properties of the Gd chelate are optimized, further enhancement of the relaxivity can be achieved by grafting the complex to macromolecules to slow molecular tumbling, thereby increasing $\tau_R$. The attachment of current commercially available contrast agents such as [Gd(DOTA)]$^{2-}$ and [Gd(DTPA)]$^{2-}$ to macromolecular constructs has been extensively studied, and in several cases, enhancements have been observed upon slowing of molecular rotation.[71-79] These contrast agents, however, are somewhat restricted because they do not have the optimal water-exchange rates that would lead to large enhancements in relaxivity. The major advantage of these aminocarboxylate-based contrast agents is their high water-solubility. For example, in the case of the attachment of multiple contrast agents to dendrimers, the solubility of the resulting macromolecule would decrease if the contrast agent has low solubility. As stated previously, solubility has generally been acknowledged as the major drawback in HOPO-based contrast agents.[64] While the choice of ligand scaffold can play a role (see section 3.2), poor solubility can be alleviated by the use of a more soluble macromolecule or by attaching the contrast agent to the interior of a soluble macromolecular vehicle.

Covalent attachment to macromolecules such as dendrimers, proteins, virus capsids, and inorganic nanoparticles, encapsulation into fullerenes, virus capsids and liposomes, non-covalent interactions with proteins, and supramolecular self assembly to form larger constructs are ideas that have been explored to build high molecular weight contrast agents.[5, 80, 81] Construction of macromolecular entities with multiple contrast agents has the advantage of increased ionic (per mM Gd) and molecular (per particle) relaxivity. The ionic relaxivity increase is due to slower molecular tumbling, and the use of multiple attachment sites leads to high molecular relaxivities. Macromolecular agents of size greater than 10 nm also have potential for application as MR angiography agents. These nano-sized particles will preferentially accumulate near lesions in vessels, but will not cross the normal healthy endothelial layer.[82] The design of macromolecules with different attachment sites for contrast agents and targeting agents is the ultimate goal in terms of imaging biological targets limited by low *in vivo* concentrations and requiring greater contrast enhancement for visualization. High-relaxivity contrast agents based on HOPO can theoretically (according to S.B.M. theory) reach the relaxivity values (up to 100 mM$^{-1}$s$^{-1}$) useful for targeted imaging and are therefore excellent candidates for attachment to macromolecules. The remainder of this section is devoted to a few representative case studies involving the construction of macromolecular HOPO-based contrast agents and their comparison to commercial contrast agents.

*HSA binding*

Non-covalent binding of contrast agents to HSA protein *in vivo* has been used to obtain contrast enhancements. The commercial agent Vasovist® (MS-325) is based on this strategy.[71, 76, 79] Binding of this contrast agent to HSA increases its circulation time in blood and also slows down its tumbling rate, leading to

greater contrast enhancements useful for blood vessel imaging. The advantage of this concept is that less material has to be injected into the patient, while the concern is the thermodynamic stability of the complex (i.e. the agent remains longer in the body depending on the binding constant between the agent and HSA).

As illustrated in the previous sections (Figure 6) heteropodal bis-HOPO-TAM ligands can be modified by the attachment of various functional groups via the terminal carboxyl group of the TAM moiety. The increase in relaxivity observed for **22** (9.1 mM$^{-1}$s$^{-1}$ from 8.8 mM$^{-1}$s$^{-1}$ at 20 MHz) upon the attachment of the PEG group is modest considering the large increase in molecular weight, both due to the decrease in $q$ and the rapid local motions in the PEG chains. The HSA-adduct of **22** afforded a relaxivity of 74 ± 14 mM$^{-1}$s$^{-1}$ at 20 MHz with a formation constant of 186 ± 50 M$^{-1}$, indicating weak binding which leads to a mixture of HSA-bound and unbound species.[49] Upon attachment of a benzyl group via the HOPO nitrogen atom (**10**), the HSA binding affinity increased to as high as 8640 ± 2000 M$^{-1}$.[50] The number of inner sphere water molecules however, is lowered to about zero (due to closer interaction with the protein), and results in relaxivities in the range of 15-19 mM$^{-1}$s$^{-1}$. For comparison, the association constant of HSA with MS-325 is 6100 ± 2130 M$^{-1}$, and the relaxivity is 50 mM$^{-1}$s$^{-1}$ at 25 MHz.[76] The interactions between HSA and the hydroxypyridonate complexes need further refinement while maintaining high $q$ values and limiting rapid local motion.
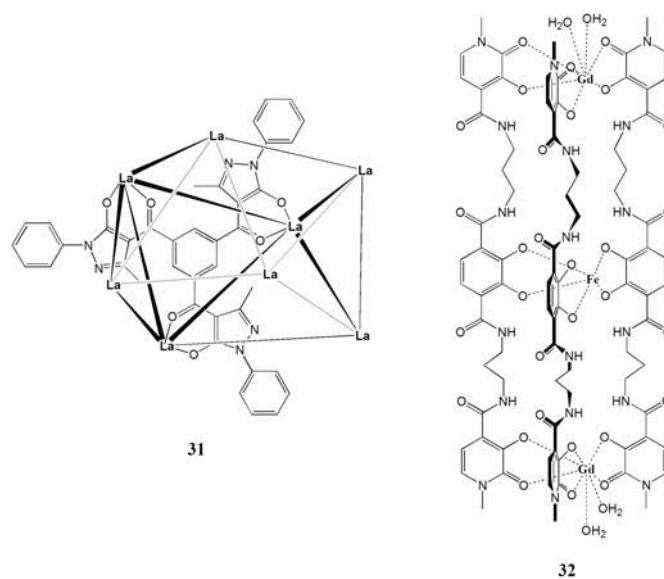


**Figure 11.** Supramolecular La based (**31**) ([La(acac)$_3$/DMSO; the coordinated DMSO molecules are omitted for clarity) and FeGd$_2$-based (**32**) constructs.

*Fe/Gd supramolecular complexes*

Self-assembly to supramolecular constructs that contain more than one Gd center can lead to high relaxivity agents due to the slower tumbling rate of the large construct. This supramolecular approach has not yielded a candidate for marketing as a practical MRI-contrast agent, however, due to difficulties in synthesis, characterization and tailoring final physiological properties of defined supramolecular Gd compounds. Many of this class of compounds also do not fulfill stability requirements because of modifications at the Gd chelating unit.

10

Supramolecular lanthanide complexes have been reviewed by Bünzli and Piguet.[83] For supramolecular d-block metals, the concept of "*incommensurate coordination number*" was developed,[84-88] a term that relates to preferred coordination geometries of metal centers and rigid ligands with a defined angle between chelating groups. Lanthanides are more flexible with regard to preferred coordination geometries than transition metals, properties that are especially important for Gd-based MRI contrast agents (which are at the border of favoring eight or nine coordinate geometries, as discussed above). The concept of *incommensurate coordination number* can thus not be transferred directly to lanthanides. Nevertheless it has been demonstrated that ligands designed along this concept can assemble into supramolecular lanthanide complexes. In most cases, the structure of those supramolecular assemblies cannot be predicted. The dominant example is the "Lord of the Rings" (**31**).[89] The $La_8L_8$ complex forms, however, instead of the analogous tetrahedron $In_6L_6$ (Figure 11). Eight lanthanum atoms occupy the eight vertices of the polyhedron, while each ligand occupies one of the eight triangular faces. Each lanthanum atom is coordinated to three ligands and each ligand binds three lanthanum atoms.

Most supramolecular constructs developed as potential MRI contrast agents are based on attaching preformed Gd[III] chelates onto tris-bidentate Fe(III) complexes. These complexes, commonly referred to as 'metallostars', can provide high relaxivity enhancements due to molecular weight increases. For example, the TTAHA (N-bis(2-aminoethyl)amine-N',N',N'',N''-tetraacetate) based metallostar has a relaxivity of 32 mM$^{-1}$s$^{-1}$ at 20 MHz.[90] To test the approach of true self-assembly, HOPO-TAM mixed ligands have been investigated, using a C3 linker between the TAM (terephthalamide) and the HOPO chelates (**32**, Figure 11).[68] The assembly reduces the tumbling of the incorporated Gd-complexes in solution, and the resulting longer rotational correlation time afforded higher relaxivities of 18.7 mM$^{-1}$ s$^{-1}$ and 23 mM$^{-1}$ s$^{-1}$ at 20 and 60 MHz respectively.

*Attachment to dendrimers and virus capsids*

Covalent attachment of contrast agents to dendrimers has been widely explored because of the advantages presented by multiple attachments and the deceleration of the tumbling rate due to molecular weight enhancement. The important restriction is that the molecule has to be rigid enough to prevent vibrational modes that allow for fast tumbling of the gadolinium containing portions.[91] Gadomer-17, a dendrimer-based contrast agent being developed by Schering, affords a 3.5 fold increase in relaxivity relative to the starting complex [Gd(DOTA)(H$_2$O)]$^-$ (16.5 mM$^{-1}$s$^{-1}$ from 4.7 mM$^{-1}$s$^{-1}$ at 20 MHz).[91] The relaxivity enhancement, however, is not as high as would be expected for the huge increase in molecular weight (40,000 Da) due to a slow water exchange rate. A single molecule of Gd-TREN-bis-HOPO-TAM-based complex grafted onto an aspartate based dendrimer (**33**, Figure 12, molecular weight 1576 g/mol,) gave a relaxivity enhancement of 1.6 times that of Gd-TREN-bis-HOPO-TAM-Me (**2**) (14.3 mM$^{-1}$s$^{-1}$ from 8.8 mM$^{-1}$s$^{-1}$ at 20 MHz). The compactness of the system and an optimal water-exchange rate allows reasonable relaxivity enhancements, despite the fact that the molecular weight increase is not as large.[92]

Virus capsids have recently been explored as potential scaffolds for attachment of Gd-chelates.[73, 77, 81, 93] Covalent attachment of TREN-bis-HOPO-TAM-based chelates onto bacteriophage MS2 capsids (90 chelates per capsid) has led to one of the highest relaxivities yet reported for these systems (Figure 12).[94] The capsid shell consists of 180 copies of the coat protein (relative molecular

mass (M$_r$) 13,700) assembled into an icosahedral arrangement (Figure 12). The diameter of this nanosized assembly is 27.4 nm, and its surfaces can be modified through lysine, cysteine or through tyrosine molecules (one per monomer on the interior surface). Both the interior and exterior surfaces of the capsid shells (devoid of RNA) were modified separately, and relaxivity enhancement depended upon the local motion of the chelate. The interior surface was modified via tyrosine moieties (**34**, relaxivity per Gd 41.6 mM$^{-1}$s$^{-1}$ and relaxivity per particle 3900 mM$^{-1}$s$^{-1}$ at 30 MHz, 25 ºC), while the exterior surface was modified via lysine residues (relaxivity per Gd 30.7 mM$^{-1}$s$^{-1}$ and relaxivity per particle 2500 mM$^{-1}$s$^{-1}$ at 30 MHz, 25 ºC). The rigidity of the linker attaching the chelate to the macromolecule clearly affects the relaxivity of the complexes, with the more rigid linkers yielding higher relaxivities.[95] Furthermore, the interior attachment strategy developed in this study has several major advantages that include solving solubility issues as well as allowing the development of targeted contrast agents via exterior surface modification.
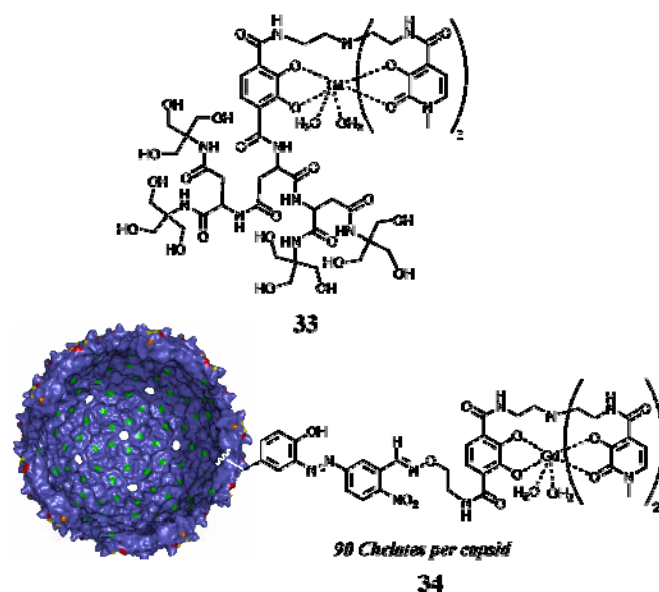


**Figure 12.** Attachment of HOPO-based contrast agents to an aspartate based dendrimer (**33**) and the internally modified MS2 virus capsid (**34**), (modified tyrosines in the interior are highlighted in green on the capsid structure[96]). The linker attaching the Gd chelate to the tyrosine is shown in the expanded structure of one of the modified tyrosines.

## 4. Conclusions

Detailed studies on lanthanide coordination chemistry have yielded exciting possibilities in the production of next-generation MRI contrast agents. While the aminocarboxylate-based agents currently in use provide some contrast enhancement, there is huge room for improvement. New ligand designs may be required to attain high relaxivity values at high magnetic field strengths to take advantage of the increased resolution made possible by new high-field instruments. Exploration of the HOPO family of Gd[III] chelates has revealed several promising platforms for consideration as practical agents, as shown in the complexes presented herein. These complexes possess the unique combination of high hydration numbers, fast water exchange rates, high stabilities, and high relaxivity values at the fields of interest. Recent work aimed at tethering the HOPO compounds to macromolecules is promising,

and further optimization of these strategies is ongoing. Regardless of the platform used, it is clear that the development of safe, high-relaxivity MRI contrast agents will remain a challenging task. With the multitude of factors that must be considered, agent design and evaluation requires a creative, multidisciplinary approach. The rewards are great, however, as improved agents would increase the breadth of possible MR applications and enhance the power of MRI as an imaging modality even further.

# References

[1]    R. B. Lauffer, *Chem. Rev.* **1987**, *87*, 901.
[2]    P. Caravan, J. Ellison, T. McMurry, R. Lauffer, *Chem. Rev.* **1999**, *99*, 2293.
[3]    É. Tóth, L. Helm, A. E. Merbach, *Top. Curr. Chem.* **2002**, *221*, 61.
[4]    R. Ranganathan, N. Raju, H. Fan, X. Zhang, M. Tweedle, J. Desreux, V. Jacques, *Inorg. Chem.* **2002**, *41*, 6856.
[5]    P. Caravan, *Chem. Soc. Rev.* **2006**, *35*, 512.
[6]    A. E. Merbach, E. Tóth, Eds., *The Chemistry of Contrast Agents in Medical Magnetic Resonance Imaging*, Wiley, Chichester, **2001**.
[7]    M. R. Goldman, T. J. Brady, I. L. Pykett, C. T. Burt, F. S. Buonanno, J. P. Kistler, J. H. Newhouse, W. S. Hinshaw, G. M. Pohost, *Circulation* **1982**, *66*, 1012.
[8]    P. C. Lauterbur, M. H. Mendoca-Dias, A. M. Rudin, *Frontier of Biological Energetics*, Academic, New York, **1978**.
[9]    E. Brücher, *Top. Curr. Chem.* **2002**, *221*, 103.
[10]   H. Gries, *Top. Curr. Chem.* **2002**, *221*, 1.
[11]   M. A. Kirchin, G. P. Pirovano, A. Spinazzi, *Invest. Radiol.* **1998**, *33*, 798.
[12]   V. M. Runge, *Crit. Rev. Diagn. Imag.* **1997**, *38*, 207.
[13]   P. Caravan, N. Cloutier, M. Greenfield, S. McDermid, S. Dunham, J. Bulte, J. Amedio, R. Looby, R. Supkowski, W. Horrocks, T. McMurry, R. Lauffer, *J. Am. Chem. Soc.* **2002**, *124*, 3152.
[14]   R. B. Lauffer, D. J. Parmelee, S. U. Dunham, H. S. Ouellet, R. P. Dolan, S. Witte, T. J. McMurry, R. C. Walovitch, *Radiology* **1998**, *207*, 529.
[15]   D. J. Parmelee, R. C. Walovitch, H. S. Ouellet, R. B. Lauffer, *Invest. Radiol.* **1997**, *32*, 741.
[16]   N. Bloembergen, *J. Chem. Phys.* **1956**, *27*, 572.
[17]   N. Bloembergen, *Phys. Rev.* **1956**, *104*, 1542.
[18]   N. Bloembergen, L. O. Morgan, *J. Chem. Phys.* **1961**, *34*, 842.
[19]   I. Solomon, *Phys. Rev.* **1955**, *99*, 559.
[20]   I. Solomon, N. Bloembergen, *J. Chem. Phys.* **1956**, *25*, 261.
[21]   S. Aime, M. Botta, M. Fasano, S. G. Crich, E. Terreno, *Coord. Chem. Rev.* **1999**, *186*, 321.
[22]   U. Baisch, D. B. Dell'Amico, F. Calderazzo, L. Labella, F. Marchetti, A. Merigo, *Eur. J. Inorg. Chem.* **2004**, 1219.
[23]   V. M. Goldschmidt, T. Barth, G. Lunde, *Skrifter Norske Videnskaps-Akademi i Oslo, I. Mat.-NaturV. Klasse* **1925**, 59.
[24]   M. Seitz, A. G. Oliver, K. N. Raymond, *J. Am. Chem. Soc.* **2007**, *129*, 11153.
[25]   J. Y. Yao, B. Deng, L. J. Sherry, A. D. McFarland, D. E. Ellis, R. P. Van Duyne, J. A. Ibers, *Inorg. Chem.* **2004**, *43*, 7735.
[26]   K. Hallenga, S. H. Koenig, *Biochemistry* **1976**, *15*, 4255.
[27]   S. H. Koenig, W. S. Schillinger, *J. Biol. Chem.* **1969**, *244*, 3283.
[28]   W. P. Cacheris, S. C. Quay, S. M. Rocklage, *Magn. Reson. Imaging* **1990**, *8*, 467.
[29]   J. F. Desreux, P. P. Barthelemy, *Nucl. Med. Biol.* **1988**, *15*, 9.
[30]   L. Helm, A. E. Merbach, *Chem. Rev.* **2005**, *105*, 1923.
[31]   Z. Jászberényi, A. Sour, É. Tóth, M. Benmelouka, A. E. Merbach, *Dalton Trans.* **2005**, 2713.
[32]   S. Laus, R. Ruloff, É. Tóth, A. E. Merbach, *Chem. Eur. J.* **2003**, *9*, 3555.
[33]   D. H. Powell, O. M. N. Dhubghaill, D. Pubanz, L. Helm, Y. S. Lebedev, W. Schlaepfer, A. E. Merbach, *J. Am. Chem. Soc.* **1996**, *118*, 9333.
[34]   É. Tóth, L. Burai, E. Brücher, A. E. Merbach, *J. Chem. Soc., Dalton Trans.* **1997**, 1587.
[35]   pGd = -log[Gd]free; [Gd]total = 1 µM, [L]total = 10 µM (pH 7.4, 25°C, 0.1 M KCl).
[36]   M. Polášek, J. Rudovský, P. Hermann, I. Lukeš, L. Vander Elst, R. N. Muller, *Chem. Commun.* **2004**, 2602.
[37]   J. Rudovský, J. Kotek, P. Hermann, I. Lukeš, V. Mainerob, S. Aime, *Org. Biomol. Chem.* **2005**, *3*, 112.
[38]   J. Costa, É. Tóth, L. Helm, A. E. Merbach, *Inorg. Chem.* **2005**, *44*, 4747.

[39]   J. Costa, R. Ruloff, L. Burai, L. Helm, A. Merbach, *J. Am. Chem. Soc.* **2005**, *127*, 5147.
[40]   R. D. Bolskar, A. F. Benedetto, L. O. Husebo, R. E. Price, E. F. Jackson, S. Wallace, L. J. Wilson, J. M. Alford, *J. Am. Chem. Soc.* **2003**, *125*, 5471.
[41]   B. Sitharaman, R. D. Bolskar, I. Rusakova, L. J. Wilson, *Nano Lett.* **2004**, *4*, 2373.
[42]   É. Tóth, R. D. Bolskar, A. Borel, G. Gonzalez, L. Helm, A. E. Merbach, B. Sitharaman, L. J. Wilson, *J. Am. Chem. Soc.* **2005**, *127*, 799.
[43]   S. Laus, B. Sitharaman, É. Tóth, R. D. Bolskar, L. Helm, S. Asokan, M. S. Wong, L. J. Wilson, A. E. Merbach, *J. Am. Chem. Soc.* **2005**, *127*, 9368.
[44]   J. Xu, S. J. Franklin, D. W. Whisenhunt, K. N. Raymond, *J. Am. Chem. Soc.* **1995**, *117*, 7245.
[45]   D. M. J. Doble, M. Melchior, B. O'Sullivan, C. Siering, J. Xu, V. C. Pierre, K. N. Raymond, *Inorg. Chem.* **2003**, *42*, 4930.
[46]   K. N. Raymond, V. C. Pierre, *Bioconjugate Chem.* **2005**, *16*, 3.
[47]   S. M. Cohen, J. D. Xu, E. Radkov, K. N. Raymond, M. Botta, A. Barge, S. Aime, *Inorg. Chem.* **2000**, *39*, 5747.
[48]   A. R. Johnson, B. O'Sullivan, K. N. Raymond, *Inorg. Chem.* **2000**, *39*, 2652.
[49]   D. M. J. Doble, M. Botta, J. Wang, S. Aime, A. Barge, K. N. Raymond, *J. Am. Chem. Soc.* **2001**, *123*, 10758.
[50]   M. K. Thompson, D. M. J. Doble, L. S. Tso, S. Barra, M. Botta, S. Aime, K. N. Raymond, *Inorg. Chem.* **2004**, *43*, 8577.
[51]   E. J. Werner, S. Avedano, M. Botta, B. P. Hay, E. G. Moore, S. Aime, K. N. Raymond, *J. Am. Chem. Soc.* **2007**, *129*, 1870.
[52]   M. K. Thompson, B. Misselwitz, L. S. Tso, D. M. J. Doble, H. Schmitt-Willich, K. N. Raymond, *J. Med. Chem.* **2005**, *48*, 3874.
[53]   W. R. Harris, K. N. Raymond, F. L. Weitl, *J. Am. Chem. Soc.* **1981**, *103*, 2667.
[54]   K. Kumar, C. A. Chang, L. C. Francesconi, D. D. Dischino, M. F. Malley, J. Z. Gougoutas, M. F. Tweedle, *Inorg. Chem.* **1994**, *33*, 3567.
[55]   R. D. Hancock, *Analyst* **1997**, *122*, R51.
[56]   R. D. Hancock, A. E. Martell, *Chem. Rev.* **1989**, *89*, 1875.
[57]   A. E. Martell, R. D. Hancock, R. J. Motekaitis, *Coord. Chem. Rev.* **1994**, *133*, 39.
[58]   B. O'Sullivan, D. M. J. Doble, M. K. Thompson, C. Siering, J. D. Xu, M. Botta, S. Aime, K. N. Raymond, *Inorg. Chem.* **2003**, *42*, 2577.
[59]   S. P. Hajela, A. R. Johnson, J. D. Xu, C. J. Sunderland, S. M. Cohen, D. L. Caulder, K. N. Raymond, *Inorg. Chem.* **2001**, *40*, 3208.
[60]   T. M. Garrett, M. E. Cass, K. N. Raymond, *J. Coord. Chem.* **1992**, *25*, 241.
[61]   T. B. Karpishin, K. N. Raymond, *Angew. Chem.* **1992**, *104*, 486; *Angew. Chem. Int. Ed.* **1992**, *31*, 466.
[62]   M. K. Thompson, M. Botta, G. Nicolle, L. Helm, S. Aime, A. E. Merbach, K. N. Raymond, *J. Am. Chem. Soc.* **2003**, *125*, 14274.
[63]   D. T. Puerta, M. Botta, C. J. Jocher, E. J. Werner, S. Avedano, K. N. Raymond, S. M. Cohen, *J. Am. Chem. Soc.* **2006**, *128*, 2222.
[64]   V. C. Pierre, M. Botta, S. Aime, K. N. Raymond, *Inorg. Chem.* **2006**, *45*, 8355.
[65]   C. J. Jocher, M. Botta, S. Avedano, E. G. Moore, J. D. Xu, S. Aime, K. N. Raymond, *Inorg. Chem.* **2007**, *46*, 4796.
[66]   V. C. Pierre, M. Melchior, D. M. J. Doble, K. N. Raymond, *Inorg. Chem.* **2004**, *43*, 8520.
[67]   C. J. Sunderland, M. Botta, S. Aime, K. N. Raymond, *Inorg. Chem.* **2001**, *40*, 6746.
[68]   V. C. Pierre, M. Botta, S. Aime, K. N. Raymond, *J. Am. Chem. Soc.* **2006**, *128*, 9272.
[69]   C. J. Jocher, E. G. Moore, J. Xu, S. Avedano, M. Botta, S. Aime, K. N. Raymond, *Inorg. Chem.* **2007**, *46*, 9182.
[70]   V. C. Pierre, M. Botta, S. Aime, K. N. Raymond, *J. Am. Chem. Soc.* **2006**, *128*, 5344.
[71]   S. Aime, M. Botta, M. Fasano, S. G. Crich, E. Terreno, *J. Biol. Inorg. Chem.* **1996**, *1*, 312.
[72]   S. Aime, M. Botta, M. Fasano, E. Terreno, *Spectrochim. Acta, Part A* **1993**, *49*, 1315.

[73]    E. A. Anderson, S. Isaacman, D. S. Peabody, E. Y. Wang, J. W. Canary, K. Kirshenbaum, *Nano Lett.* **2006**, *6*, 1160.

[74]    V. Comblin, D. Gilsoul, M. Hermann, V. Humblet, V. Jacques, M. Mesbahi, C. Sauvage, J. F. Desreux, *Coord. Chem. Rev.* **1999**, *186*, 451.

[75]    J. B. Livramento, A. Sour, A. Borel, A. E. Merbach, V. Toth, *Chem. Eur. J.* **2006**, *12*, 989.

[76]    R. N. Muller, B. Raduchel, S. Laurent, J. Platzek, C. Pierart, P. Mareski, L. Vander Elst, *Eur. J. Inorg. Chem.* **1999**, 1949.

[77]    D. E. Prasuhn, R. M. Yeh, A. Obenaus, M. Manchester, M. G. Finn, *Chem. Commun.* **2007**, 1269.

[78]    J. Rudovsky, M. Botta, P. Hermann, K. I. Hardcastle, I. Lukes, S. Aime, *Bioconjugate Chem.* **2006**, *17*, 975.

[79]    S. G. Zech, H. B. Eldredge, M. P. Lowe, P. Caravan, *Inorg. Chem.* **2007**, *46*, 3576.

[80]    M. Bottrill, L. Kwok, N. J. Long, *Chem. Soc. Rev.* **2006**, *35*, 557.

[81]    G. M. Nicolle, E. Toth, K. P. Eisenwiener, H. R. Macke, A. E. Merbach, *J. Biol. Inorg. Chem.* **2002**, *7*, 757.

[82]    H. E. Daldrup-Link, R. C. Brasch, *Eur. Radiol.* **2003**, *13*, 354.

[83]    J. C. G. Bunzli, C. Piguet, *Chem. Rev.* **2002**, *102*, 1897.

[84]    M. Albrecht, *Angew. Chem.* **1999**, *111*, 3671; *Angew. Chem. Int. Ed.* **1999**, *38*, 3463.

[85]    M. Albrecht, M. Schneider, H. Rottele, *Angew. Chem.* **1999**, *111*, 512; *Angew. Chem. Int. Ed.* **1999**, *38*, 557.

[86]    D. L. Caulder, C. Bruckner, R. E. Powers, S. Konig, T. N. Parac, J. A. Leary, K. N. Raymond, *J. Am. Chem. Soc.* **2001**, *123*, 8923.

[87]    D. L. Caulder, K. N. Raymond, *J. Chem. Soc., Dalton Trans.* **1999**, 1185.

[88]    D. L. Caulder, K. N. Raymond, *Acc. Chem. Res.* **1999**, *32*, 975.

[89]    J. Xu, K. N. Raymond, *Angew. Chem.* **2000**, *112*, 2857; *Angew. Chem. Int. Ed.* **2000**, *39*, 2745.

[90]    J. B. Livramento, E. Toth, A. Sour, A. Borel, A. E. Merbach, R. Ruloff, *Angew. Chem.* **2005**, *117*, 1504; *Angew. Chem. Int. Ed.* **2005**, *44*, 1480.

[91]    G. M. Nicolle, E. Toth, H. Schmitt-Willich, B. Raduchel, A. E. Merbach, *Chem. Eur. J.* **2002**, *8*, 1040.

[92]    V. C. Pierre, M. Botta, K. N. Raymond, *J. Am. Chem. Soc.* **2005**, *127*, 504.

[93]    M. Allen, J. W. M. Bulte, L. Liepold, G. Basu, H. A. Zywicke, J. A. Frank, M. Young, T. Douglas, *Magn. Reson. Med.* **2005**, *54*, 807.

[94]    J. M. Hooker, A. Datta, M. Botta, K. N. Raymond, M. B. Francis, *Nano Lett.* **2007**, *7*, 2207.

[95]    A. Datta, J. M. Hooker, M. Botta, M. B. Francis, S. Aime, K. N. Raymond, *J. Am. Chem. Soc.* **2008**, *130*, 2546.

[96]    K. Valegard, L. Liljas, K. Fridborg, T. Unge, *Nature* **1990**, *345*, 36.